International Conference on Space Optics—ICSO 2022

Dubrovnik, Croatia

3–7 October 2022

Edited by Kyriaki Minoglou, Nikos Karafolas, and Bruno Cugny,

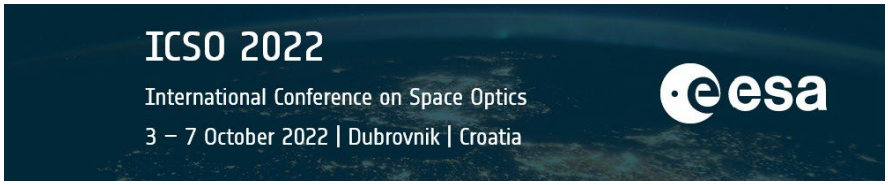

Evaluation of radiation hardness of InP-based Photonic Integrated Circuits for space applications

International Conference on Space Optics — ICSO 2022, edited by Kyriaki Minoglou, Nikos Karafolas, Bruno Cugny, Proc. of SPIE Vol. 12777, 127776F · © 2023 ESA and CNES · 0277-786X · doi: 10.1117/12.2691127

Evaluation of radiation hardness of InP-based Photonic Integrated Circuits for space applications

Antonio Pérez-Serrano*[a], Alicia Soria-Gómez[a], David Poudereux[b], Juan Barbero[b], Luc Augustin[c], José Manuel G. Tijero[a], and Ignacio Esquivias[a]
[a] Universidad Politécnica de Madrid, ETSI Telecomunicación-CEMDATIC, Madrid, Spain; [b] Alter Technology TÜV Nord S.A.U., Tres Cantos, Madrid, Spain; [c] SMART Photonics, Eindhoven, The Netherlands

ABSTRACT

In this work we present experimental results on the radiation hardness of InP based Photonic Integrated Circuits (PICs) fabricated in a multi-project wafer through an open access platform. The PIC includes different types of building blocks: semiconductor optical amplifiers (SOA), waveguides, electro-optical phase modulators (EOPM), multi-mode interference couplers and photodiodes (PD). Three chips were submitted to gamma radiation up to 106 krad in four steps and another three to proton radiation up to 1.5 x 1011 p+/cm2. The effects of the radiation were evaluated by measuring on-wafer the power-current-voltage (P-I-V) characteristics and emission spectra of several tunable four-section Distributed Bragg Reflector (DBR) lasers. The P-I-V characteristics measured before radiation showed kinks corresponding to modal changes and stable regions with single longitudinal mode emission. After the radiation some changes were observed: i) the value of the threshold current in some of the lasers, either increasing or decreasing its value; ii) slightly different emission wavelength and evolution of the modal jumps with current. However, these changes were not systematic in all devices, and they were not dependent of the radiation dose. In consequence, they were attributed to the lack of reproducibility of the on-wafer measurements and the high sensitivity of the modal selection to temperature changes in these DBR lasers. In conclusion, the building blocks of the PICs involved in the DBR laser (SOA, EOM, waveguide, PD) can be considered radiation hard up to the levels in the tests, which were typical for space applications.

Keywords: Photonic Integrated Circuits, InP-based semiconductor lasers, Distributed Bragg Reflector lasers, radiation hardness, space applications

1. INTRODUCTION

InP-based Photonic Integrated Circuits (PIC) are continuously expanding their application range in sensing, communication, and computing [1, 2]. They offer enormous advantages in terms of size, weight, scalability, and reduction of mounting complexity in comparison with systems based on discrete components. In the last decade, the PIC technology has received a major boost with the introduction of generic integration platforms [3, 4]. Generic photonic integration adapts the model of microelectronics, where a wide variety of circuits can be created with a limited set of predefined building blocks, fabricated in the same integration process. In InP-based PICs, these basic building blocks are waveguides, couplers, amplifiers, detectors, and modulators, that can be integrated into more complex sub-circuits. Generic integration presents some advantages. Using standardized industrial integration processes, stable and reproducible performance is achieved. In addition, because the building blocks are predefined, circuit design can be done at the functional level, allowing a more efficient design flow. These advantages are especially relevant for space applications and in consequence there is a high interest in the evaluation of these components in space environment. A recent review on the performance of PICs for space applications can be found in [5]. Different types of InP-based devices, such as laser diodes [6, 7], rib waveguide resonators [8], and Mach-Zehnder modulators [9] have been tested in space environments, but as far as we know the evaluation of a complete chip with a combination of building blocks has not yet been reported.

*antonio.perez.serrano@upm.es

In this work we present experimental results on the radiation hardness of InP based PICs fabricated using multi-project wafers through open access platforms. The PICs include different types of building blocks: semiconductor optical amplifiers (SOA), waveguides, electro-optical phase modulators (EOPM), multi-mode interference couplers and photodiodes (PD). We report the evolution of the emission properties of several Distributed Bragg Reflector (DBR) lasers after proton and gamma radiation campaigns.

2. DESCRIPTION OF THE PHOTONIC INTEGRATED CIRCUITS

The PICs have been fabricated by SMART Photonics through the open access platform JePPIX (Joint European Platform for Photonic Integration of Components and Circuits). The initial design and simulations were performed using VPIphotonics Design Suite and the layout was created with Nazca Design. Fig. 1 a) shows a photograph of the fabricated device, with dimensions 4x4.6 mm^2, and Fig. 1b) shows the layout. It includes several types of lasers: 4-section DBR lasers, ring lasers and widely tunable laser with three intracavity Mach–Zehnder interferometers. Four DBR lasers were selected for this work, named as laser-6, -7, -8 and -9 in the labeled region of Fig. 1b). Each laser has four sections: a front DBR, a SOA, an EOPM, and a back DBR, as it is shown in the schematics of Fig 2., with lengths 50 μm, 400 μm, 200 μm, and 250 μm, respectively. The sections are electrically isolated through 30 μm long p-etched regions. The output of the back DBR is connected to an internal PD. The pitches of both DBRs of laser-6, -7, -8, and -9 have been designed for Bragg wavelengths of 1550 nm, 1544 nm, 1560 nm, and 1570 nm, respectively. The chips were not packaged, and they were contacted by using DC needles (see Fig. 1a). The backside of the chip acts as a common ground for all blocks.

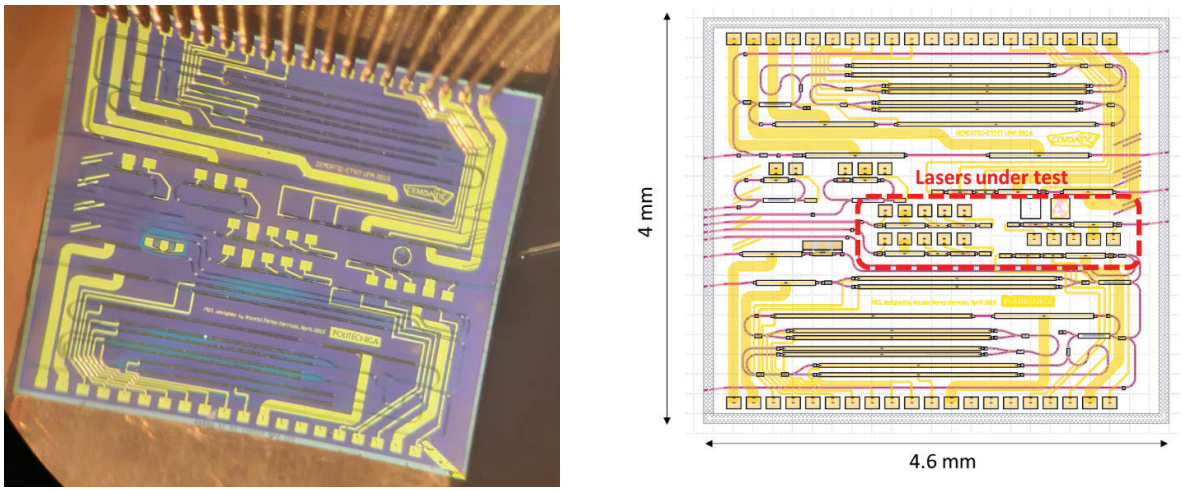

Figure 1. a) photograph of the PIC; b) layout of the PIC

3. RADIATION CONDITIONS

Three chips were submitted for Total Ionization Dose (TID) or gamma radiation test in Centro de Investigaciones Energéticas, Medioambientales y Tecnológicas (Madrid, Spain) up to 105.9 Krad(Si) in five steps. Table 1 summarizes the dose, accumulate dose and time for each step. After each radiation step a temporal window of two hours allowed the characterization of several lasers. Other three chips were submitted for Displacement Damage (DD) test with proton radiation up to $1.5 \cdot 10^{11}$ proton/cm^2 at 60MeV. The Power-Current (P-I) and Voltage-Current (V-I) characteristics and emission spectra as a function of the current of 7 lasers submitted for gamma radiation and 8 lasers submitted for proton radiation were measured before and after the radiation process.

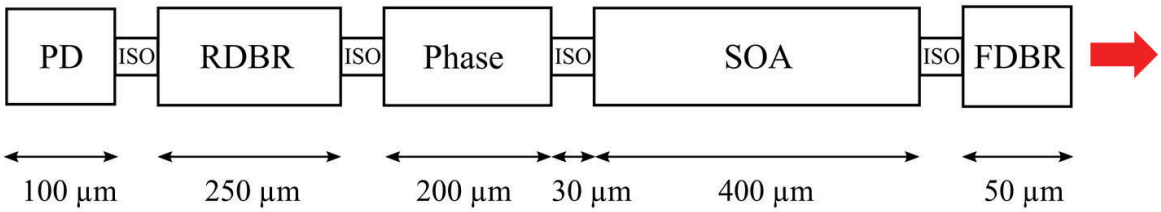

Figure 2. Schematics of the DBR lasers

Table 1. Dose rate, dose, accumulated dose, and duration of each gamma radiation step.

Step	Dose rate rad(Si)/h	Dose krad(Si)	Accum. Dose krad(Si)	Time
0	360.8	1.35	1.35	3 h 8 min
1	225	9.22	10.57	1 d 7 h
2	225	21.15	31.42	3 d 22 h
3	225	20.92	52.34	3 d 21 h
4	225	53.54	105.88	9 d 22 h

4. RESULTS

Fig. 3 shows the P-I characteristics of one of the lasers submitted to gamma radiation during the windows between radiation steps, measured using the external (Fig. 3a) and internal (Fig. 3b) photodiodes. The external power was measured by coupling the output light into a lensed optical fiber and measuring the photocurrent in a Ge photodiode. The differences in power observed in the external photodiode are simply due to the different coupling losses from the PIC to the external fiber. Each P-I curve shows small kinks due to modal changes, as it will be shown later when analyzing the spectra. These changes of modes are attributed to the thermal shifts of the FabryPerot (FP) modes and of the Bragg wavelengths of both DBRs when the SOA current is increased. As the heat is produced at the SOA and it diffuses towards the DBRs, the temperature increase of the SOA is different to that of the DBRs, giving rise to small differences in the losses of each mode, and in consequence to modal jumps. When comparing the P-I curves measured during the different radiation windows, slight differences in the position of the modal jumps can be observed, but the threshold current and power level (measured in the internal photodiodes) are basically constant. These small changes are attributed to highly critical threshold conditions in these DBR lasers, in which a modal jump can be produced by minute changes in the temperature or driving conditions, rather than to effects of the radiation. This is confirmed by the slight variations of the threshold current in the different windows, shown in table 2, attributed to modal changes, which do not show any clear trend with the accumulated radiation dose. In fact, similar changes in the P-I curves have been observed for different measurements of the same device by simply removing the chip and contacting it again.

Table 2. Evolution of the threshold current of one of the gamma radiated lasers measured during the windows between radiation steps. The threshold current is calculated from the first linear part of the P-I characteristic, before the first kink appears.

	Initial	Window1	Window2	Window3	Window4
I_{th} (mA)	31.0	31.2	32.5	30.6	30.1

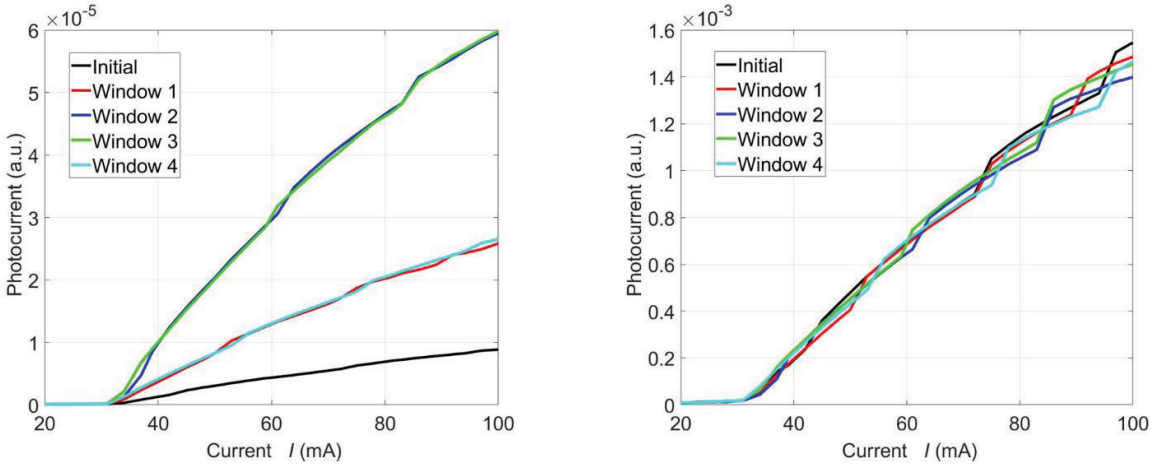

Figure 3. Photocurrent measured in the external photodiode (a) and in the internal photodiode (b) vs. injected current for a laser before and after the different steps of gamma radiation (see table I)

Fig. 4 shows the map of the emission spectra of one of the lasers submitted to gamma radiation before radiation (Fig. 4a) and after the total radiation dose (Fig. 4b), as a function of the current injected in the SOA section. The spectra were measured with an Optical Spectrum Analyzer (OSA) with 0.05 nm resolution. The spectral map clearly shows the FP modes separated 0.41 nm, corresponding to a Free Spectral Range (FSR) of 51.2 GHz given by the cavity length of ~900 μm, which is reasonable considering the effective lengths of the DBRs. A FP modal jump can be observed in Fig. 4a) at around 37 mA, but other smaller jumps of around 0.03 nm can be also observed at ~ 42 mA, 75 mA and 95 mA. These small jumps are attributed to feedback from the interior of the chip, as they correspond to the cavity length of the ring laser (~ 1.2 cm) which is connected to the DBR laser as it can be seen in Fig. 1b). It is well known that coupled cavity effects can produce unexpected modal jumps [10]. The red shift of the FP modes above threshold when increasing the current in Fig. 4 is due to thermal effects as the effective index increases with temperature, while the blue shift below threshold is due to the increase of carrier density, as the effective index decreases with the carrier density. When comparing the spectral maps before and after radiation (Fig. 4) minor differences are observed, which are not attributed to radiation effects but to the high sensitivity of modal competition with driving conditions.

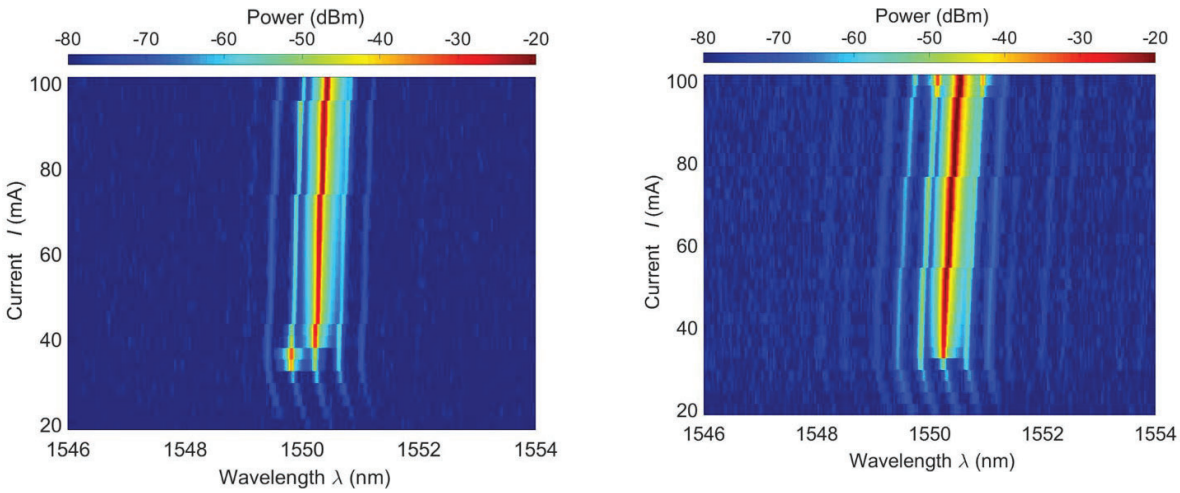

Figure 4. Map of the emission spectra as a function of the injected current for a laser of PIC1 ~~previously~~ before (a) and after the total dose of gamma radiation.

Table 3 shows the threshold currents of the seven lasers submitted to gamma radiation, before and after the total radiation dose. Small differences can be observed, and in most of the lasers the threshold current after radiation is higher than before, but there is not a systematic degradation attributable to radiation effects.

Table 3. Threshold current of the seven gamma radiated lasers measured after and before radiation. The threshold current is calculated from the first linear part of the P-I characteristic, before the first kink appears. The name of the laser is given as X_Y, where X is the chip number and Y the laser number.

Laser	4_6	4_7	4_8	6_6	6_8	7_7	7_8
I_{th} (mA) (Before)	31	25.0	22.7	24.3	27.5	33.9	29.7
I_{th} (mA) (After)	30.1	25.5	23.5	25-9	28.3	35.2	30.9

Fig. 5 shows an example of the P-I (a) and V-I (b) characteristics of one of the lasers submitted to proton radiation. Small differences in both characteristics before and after radiation can be observed, but again they are not attributable to radiation but to modal changes. The measured threshold currents of the eight lasers submitted to proton radiation, before and after radiation are shown in Table 4. Again, small differences can be observed, and three lasers present a reduced threshold current after radiation, again indicating that there is not a systematic degradation attributable to radiation effects. The spectra of the lasers submitted to proton radiation (not shown) also present small modal changes but not important differences before and after radiation.

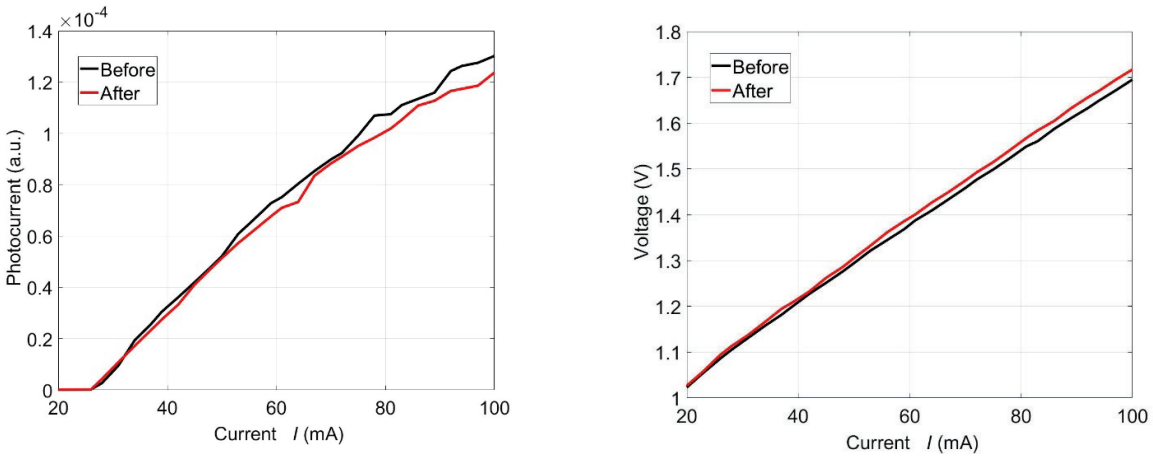

Figure 5. Photocurrent measured in the internal photodiode (a) and laser voltage (b) vs. injected current for a laser before (black) and after(red) proton radiation

Table 4. Threshold current of the eight proton radiated lasers measured after and before radiation. The threshold current is calculated from the first linear part of the P-I characteristic, before the first kink appears. The name of the laser is given as X_Y, where X is the chip number and Y the laser number.

Laser	3_6	3_7	3_8	5_6	5_7	5_8	5.9	8_8
I_{th} (mA) (Before)	26.7	30.0	29.1	25.9	26.9	27.0	29.1	36.9
I_{th} (mA) (After)	27.2	26.3	30.5	25.1	25.6	27.4	30.4	37.4

5. CONCLUSIONS

We have evaluated the radiation hardness of InP-based PICs for space applications by measuring the power-current characteristics and spectral response of several DBR lasers fabricated in an open access platform in a multi-project wafer before and after being submitted to gamma or proton radiation. The results indicate that the PICs do not suffer degradation due to the radiation effects, although there are small differences between the initial and final measurements attributed to the on-wafer characterization system and to critical dependence of the modal selection mechanism on the operation conditions. We conclude that the building blocks of the PICs involved in the DBR laser (SOA, EOM, waveguide, PD) can be considered radiation hard up to the levels in the tests, which were typical for space applications.

6. ACKNOWLEDGEMENTS

This work has been supported by Ministerio de Ciencia e Innovación of Spain (LIDERA, RTI2018-094118-B-C21), Comunidad de Madrid and FEDER Program under grant SINFOTON2-CM (S2018/NMT-4326), and Cátedra Alter Technology Desarrollo e Innovación en Fotónica, ETSI Telecomunicación - Universidad Politécnica de Madrid.

REFERENCES

[1] S. Arafin and L. A. Coldren, “Advanced InP photonic integrated circuits for communication and sensing,” IEEE J. Sel. Topics Quantum Electron., 24(1), 6100612, (2018).

[2] F. Kish et al., “System-on-chip photonic integrated circuits,” IEEE J. Sel.Topics Quantum Electron., 24(1), 6100120 (2018).
[3] M. Smit et al., “An introduction to InP-based generic integration technology”, Semicond. Sci. Technol. 29(8), 083001 (2014).
[4] L. M. Augustin et al., “InP-based generic foundry platform for photonic integrated circuits,” IEEE J. Sel. Topics Quantum Electron., 24(1), 6100210 (2018).
[5] WANG, XingJun, et al. "Integrated photonics for space applications." SCIENTIA SINICA Physica, Mechanica & Astronomica 51(2), 024201 (2021).
[6] Johnston A H. “Radiation effects in optoelectronic devices”, IEEE Trans. Nucl. Sci. 60(3), 2054–2073 (2013).
[7] Adamiec, P., et al. "Radiation tests on semiconductor optical sources for space applications." International Conference on Space Optics—ICSO 2016, Proc. SPIE 10562, 174-182 (2017).
[8] Brunetti, Giuseppe, et al. "Measured radiation effects on InGaAsP/InP ring resonators for space applications." Optics Express 27(17), 24434-24444 (2019).
[9] Gajanana, Deepak, et al. "Irradiation tests on InP based Mach Zehnder modulator." Journal of Instrumentation (02), C02025 (2013).
[10] Pérez-Serrano, Antonio, et al. "Wavelength Jumps and Multimode Instabilities in Integrated Master Oscillator Power Amplifiers at 1.5 μm: Experiments and Theory." IEEE Journal of Selected Topics in Quantum Electronics 21(6), 315-323 (2015).